We are IntechOpen, the world's leading publisher of Open Access books Built by scientists, for scientists

6,900
Open access books available

186,000
International authors and editors

200M
Downloads

Our authors are among the

154
Countries delivered to

TOP 1%
most cited scientists

12.2%
Contributors from top 500 universities

WEB OF SCIENCE™

Selection of our books indexed in the Book Citation Index in Web of Science™ Core Collection (BKCI)

Interested in publishing with us?
Contact book.department@intechopen.com

Numbers displayed above are based on latest data collected.
For more information visit www.intechopen.com

Chapter

Effects of Mass-Loading on Performance of the Cyclone Separators

Vikash Kumar and Kailash Jha

Abstract

The concentration of dust particles in the incoming air has a significant effect on the performance of cyclone separators. In the proposed work, four particle concentrations (0.05, 0.1, 0.2 and 0.3 kg/kg) in the dust stream have been mathematically investigated using both one-way and two-way coupling. A fine grid is solved using the Large Eddy Simulations to capture the accurate physical phenomena. For vortices smaller than the grid size the Smagorinsky Lilly model with a Smagorinsky constant, C_s of 0.1 has been applied. The collection efficiencies of the four cases are presented and the differences between the one-way and two-way coupled simulation approaches are highlighted in the present study. The two-way coupled simulations show an increase in the collection efficiency from 62% to 70% on increasing the solid loadings from 0.05 to 0.3 with marginal increase in pressure drop of 4.8%.

Keywords: stairmand high-efficiency cyclone, computational fluid dynamics, large Eddy simulations, solid loadings, Eulerian-Lagrangian

1. Introduction

Petrochemical, cement, mineral, powder processing industries, use cyclone separators extensively for separating or filtering fine particles from the primary phase. They are also used in boilers for recovery of particulate fuel, in vacuum cleaners and in biomedical applications for filtering microscopic bacteria from the air. In industries all over the world, cyclone separators are subjected to a variety of operating conditions at which they need to work efficiently. Therefore developing an understanding of the relation between performance and the operating conditions is important. The operating conditions mentioned here refer to the velocity, temperature of the incoming dust-laden air and the size distribution, the concentration of the particulate matter suspended in the air stream. The performance of the cyclone separator is represented by two parameters, firstly the pressure loss across the cyclone, (its dimensionless form being the Euler number) and secondly its collection efficiency over the range of particle diameters (dimensionless form being the Stokes number), fed into the cyclone. This is presented in the form of a curve plotted between the particle diameter (Stokes number) and its collection efficiency known as the grade efficiency curve. This curve brings into the picture a new parameter known as the cut-size diameter Stk_{50} which has been used extensively to provide a sense of the collection efficiency of a cyclone separator. The cut-size

diameter is the particle diameter that corresponds to 50% collection efficiency on the grade efficiency curve. Physically it means that for the given operating conditions and the particular cyclone separator, particle diameters lesser than the cut-size will have less than 50% of the incoming solids getting collected in the dustbin. Whereas more than 50% of the larger particle diameters will be collected in the dust bin. This is observed in cyclone separators as the heavier particles have greater inertia and are more prone to separate from the swirling flow in the cyclone separator and move towards the walls. But the lesser diameter particles tend to move with the flow and are hence very difficult to separate. This behavior which determines whether a particle will be heavy enough to separate from the flow or be light enough to follow the flow depends on the drag exerted on the particle by the airflow and the Reynolds number of the flow. As the Reynolds number of the flow is same for all the particle sizes, the drag emerges as an important factor and is dependent on the diameter and roughness of the particle as suggested earlier that the grade efficiency curve is a function of the particle size.

Research suggests that apart from particle size, the grade efficiency curve or simply the collection efficiency for different particle sizes also shows a variation with the particle concentration inside the cyclone separator. Hoffmann et al. [1] experimented three cyclone models with different vortex finder diameters at three different inlet velocities and presented the variation of the two performance parameters with respect to solids loadings (0–0.04 kg/m^3). The relation between separation efficiency and vortex finder diameter was found to be inversely proportional as reported by Brar et al. [2]. The separation efficiency improved with inlet velocity but only up to a certain solid loading, after which the reverse was seen. They concluded that an increase in solid loadings reduced the pressure drop slightly and increased the overall collection efficiency. An interesting point observed was that at lower inlet velocity (10 m/s) the improvement in efficiency due to an increase in solid loadings was higher than that at higher inlet velocity (20 m/s). The curves crossed at a solid loading of 0.02 kg/m^3. A similar observation of obtaining a higher collection efficiency at 18 m/s than at 27 m/s was reported by Fassani and Goldstein [3] who conducted experiments at solid loadings as high as 20 kg of solids/kg of gas. They further reported that dust-laden air showed lower pressure drop values than that of dust-free air, collection efficiency improved with solid loadings up to 12 kg of solids/kg of gas, after which reduction in efficiency was seen.

It has been reported that two-way coupling simulations are necessary beyond a certain solid loading threshold to capture the reductions in the swirl [4]. It has also been reported that if the cyclone separator load exceeded the critical load [1], improvements in separation performance would be seen. The present paper performance analysis of the Stairmand High-Efficiency Cyclone (SHEC) at four different solid loadings with the help of one way and two-way coupled Large-eddy Simulations. Both one way and two-way coupled simulations are performed to enquire if they can capture the reduction in swirl and the improvements in separation performance at solid loadings of 0.05, 0.1, 0.2 and 0.3 (kg of dust per kg of air). Many studies on the effect of mass loadings on the efficiency of cyclone separators are available in literature such as [1, 4–6]. But the upper limit of the range studied in most of them is only 0.1 kg of dust per kg of air, whereas Derksen et al. [7] investigated the effects on the flow up to the range of 0.2. Although the solids loading of 0.2 has been investigated by Derksen et al. [7] the authors stated that as the simulations were computationally expensive, they could not perform extended simulations to get quantitative results on various quantities. The present paper extends the upper limit of solid loadings to 0.3 and performs a comparison of one way and two-way coupled simulation strategies. The validation of the clean gas flow

pattern with experimental data [8] has been done, this helps emphasize the particle modeling approach and its accuracy.

2. Numerical simulations

The present gas-particle simulations are performed using the Eulerian-Lagrangian approach, the gas flow field is determined using a Eulerian approach and the particles' trajectories are calculated using a Lagrangian approach. The fluid medium is considered as a continuum for which the Navier-Stokes equation pertaining to the coordinate directions is solved and the particle or dispersed phase trajectories are tracked in the developed gas flow field. The particle equation of motion is used to calculate the particle velocity from the instantaneous gas velocity.

2.1 Gas flow

The gas flow inside the cyclone separator is modeled using Large Eddy Simulations (LES), which has been successfully applied to flows involving cyclone separators [9–15]. LES has the potential to resolve most of the energy-carrying larger eddies directly, whereas smaller energy eddies are modeled using a sub-grid scale (SGS) model. The sub-grid scale refers to scales smaller than the grid size. As the grid size determines the scales of eddies that will be directly resolved, a smaller grid size results in higher accuracy at the cost of higher computational time. The Smagorinsky-Lilly model [16] with a Smagorinsky constant of 0.1 has been used for modeling the sub-grid scale stresses. The sub-grid scale stresses are calculated employing the Boussinesq hypothesis [17] similar to that in the Reynolds averaged Navier-Stokes (RANS), model.

As turbulence introduces erratic velocity fluctuations in the flow field, appropriate models are needed to capture the turbulent characteristics of the physical flow field into the numerical calculations. Many models have been developed over time to approximate the turbulent behavior of fluids, Spalart-Allmaras model, k-ε model and k-ω models are some that use the Boussinesq hypothesis. These models are relatively less expensive in a computational sense but possess shortcomings in many complex flows. Reynolds Stress equation model is another approach of modeling turbulence which uses three additional equations for determining the Reynolds stresses is considered in the present study. Accuracy of the Reynolds Stress model in the context of flows in cyclone separators has been well established in the literature. The Reynolds averaged continuity and Navier-Stokes equations are given as [2]:

$$\frac{\partial \overline{u_i}}{\partial x_i} = 0 \tag{1}$$

$$\frac{\partial \overline{u_i}}{\partial t} + \overline{u_i}\frac{\partial \overline{u_j}}{\partial x_j} = -\frac{1}{\rho}\frac{\partial \overline{P}}{\partial x_i} + \nu\frac{\partial^2 u_i}{\partial^2 x_j} + \frac{\partial}{\partial x_j}\tau_{ij} \tag{2}$$

where $\overline{u}$ is the mean velocity, x is the coordinate direction, $\overline{P}$ the average static pressure, ρ the gas density, ν the kinematic viscosity and τ_{ij} the Reynolds stress tensor ($\tau_{ij} = -\overline{u_i' u_j'}$) with u' as the fluctuating component of velocity, this term represents the transfer of momentum due to turbulence. Eq. (1) is the differential form for the conservation of mass for a small fluid element whereas Eq. (2) is the

differential form for the conservation of momentum. The terms on the left hand side of Eq. (2) collectively describe the acceleration of a fluid element, the first term denoting the temporal acceleration and the second denoting the convective acceleration. The terms on the right hand side represent the pressure force, viscous force and the Reynolds stress tensor.

2.2 Particle motion

The particle motion inside the cyclone separator is described using a Lagrangian approach, the equation for motion of the particle is given by Clift et al. [18]:

$$\frac{\partial u_{pi}}{\partial t} = F_D\left(u_i - u_{pi}\right) + \frac{\left(\rho_p - \rho\right)g_i}{\rho_p} + F_i \tag{3}$$

Where u_{pi} is the particle velocity, first term on the right-hand side, denotes the drag force encountered by the particles due to fluid flow, the second term denotes forces due to gravitational accelerations and the third term includes all the additional forces that can be accounted for. The additional force in Eq. (3) comprises of virtual mass force, the pressure gradient force, the Brownian force and the Saffman's lift force some of which can be safely neglected for the case of particulate flow in cyclone separators [19]. The particle trajectories in the turbulent flow are solved by using the gas velocity derived from the gas flow field computed by the Large Eddy Simulations. The particles considered are small and interpenetrating in nature, which means the collisions between the particles are neglected in the present simulations. In cases where the particle concentration inside the cyclone separator is small, the exchange of momentum from the dispersed phase to the fluid phase can be neglected, this is known as a one way coupled simulation. Whereas when the exchange of momentum from the dispersed phase to the fluid phase becomes significant and is accounted for in the simulations, it is known as a two-way coupled simulation. In the present study, both one way and two-way coupled simulations have been employed. The effects of turbulence on the particles are incorporated using a discrete random walk model [20], this model simulates the interaction of the particles with discrete stylized fluid phase turbulent eddies. The turbulent eddies are characterized by Gaussian distributed random velocity fluctuations and the eddy time scale. Assuming anisotropy of the stresses, the instantaneous turbulent velocity fluctuations are given as [20]:

$$u_i^{'} = \xi\sqrt{\overline{u_i^{'2}}} \tag{4}$$

Each interaction of the particle with the turbulent eddy, is considered over a time scale which is shorter of the eddy time scale and the eddy crossing time, given by:

$$\tau_e = -T_L \ln\left(r\right) \tag{5}$$

Where r is a random number between 0 and 1 and T_L is given by:

$$T_L \approx 0.15\frac{k}{\varepsilon} \tag{6}$$

2.3 Cyclone geometry

The cyclone geometry considered in the present study is the Stairmand High-Efficiency Cyclone [21], same as that used by Hoekstra [8] in experiments and by Derksen et al. [4] in large-eddy simulations using the lattice-Boltzmann discretization scheme. The choice of cyclone geometry is made keeping in mind the experimental data available facilitating validation of the simulation procedure. The cyclone geometry used for the simulations is presented in **Figure 1**. A similar obstruction with diameter 0.36 D_{exit} has been provided slightly upstream of the outflow boundary in the present geometry in order to prevent subcritical flow [11].

2.4 Discretization of the solution domain

The cyclone geometry has been meshed using ICEM CFD, a meshing tool which comes along the Ansys commercial software package which uses the multi-block meshing approach. The domain is meshed using high-quality hexahedral elements

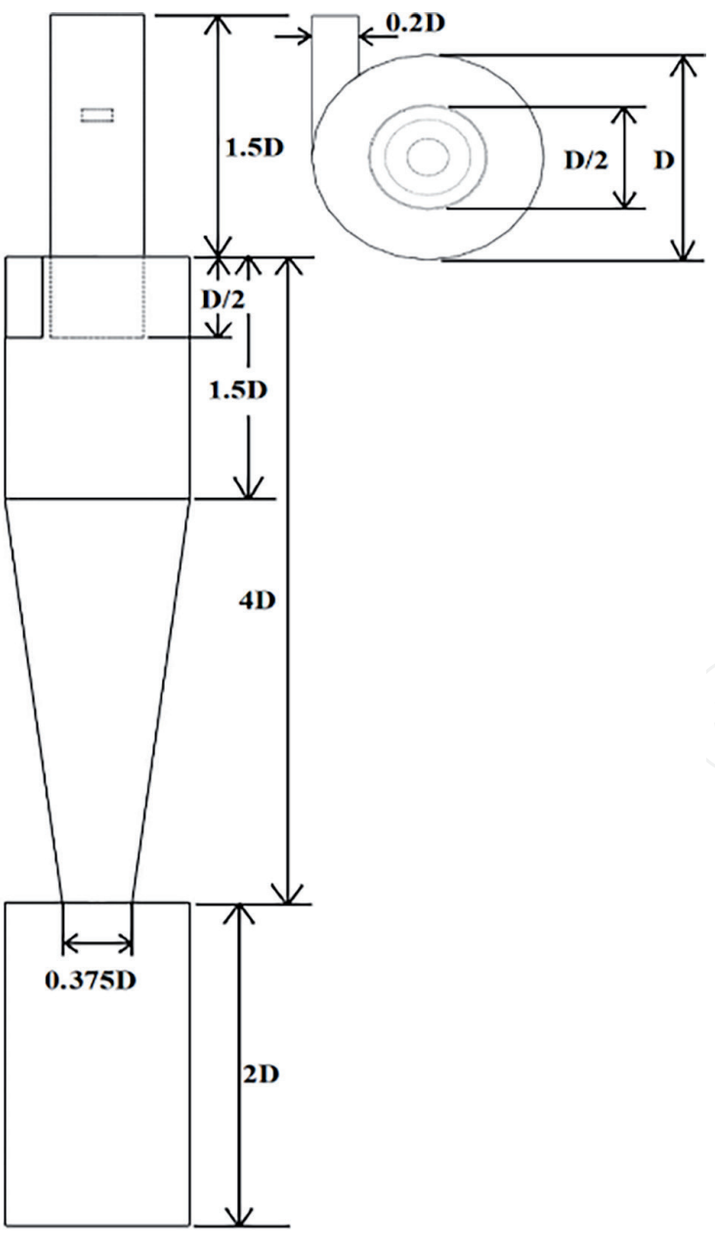

Figure 1.
Cyclone dimensions D = 0.29 m.

with the lowest element orthogonality being 0.06 and highest element aspect ratio being 31.12. For the case of LES, a small value of Δx should be used in order to minimize the small scale energy-carrying eddies. However, this can lead to a high computational cost therefore a compromise has to be made, keeping in mind the steep velocity gradients in the boundary layer. The value of Δx is taken as D/90 on the innermost block taken from [11] resulting in approximately 2×10^6 elements.

2.5 Solver settings

The present simulations have been carried on the commercial software Ansys Fluent v15.0. A pressure-based transient simulation has been conducted to capture the fluid flow inside the cyclone separator. For capturing the effects of turbulence, the Reynolds stress model with a linear pressure-strain relationship is employed, standard wall functions based on the works of Launder and Spalding [22] are used for treating the boundary layer flow. For the gas flow, air with a density of 1.225 kg/m^3 and dynamic viscosity of 1.7894×10^{-5} kg/m-s and inlet velocity of 16.1 m/s which corresponds to a Reynolds number of 28×10^5 has been taken. The inlet velocity is the same as that taken by Hoekstra [8] in experiments and by Derksen et al. [4] in simulations. The boundary conditions for the fluid phase has been specified as velocity-inlet at the inlet, outflow at the outlet and all other surfaces has been defined as walls. For the dispersed phase, the inlet boundary is prescribed as an escape for the particles, the bottom of the dustbin is prescribed as a trap and the remaining surfaces are considered as walls. The walls are set to reflect the particles with normal and tangential wall reflection coefficients as 1, facilitating elastic collisions between the walls and particles.

The discretization schemes used for pressure velocity coupling is SIMPLEC (Semi-Implicit Method for Pressure Linked Equations-Consistent), the pressure

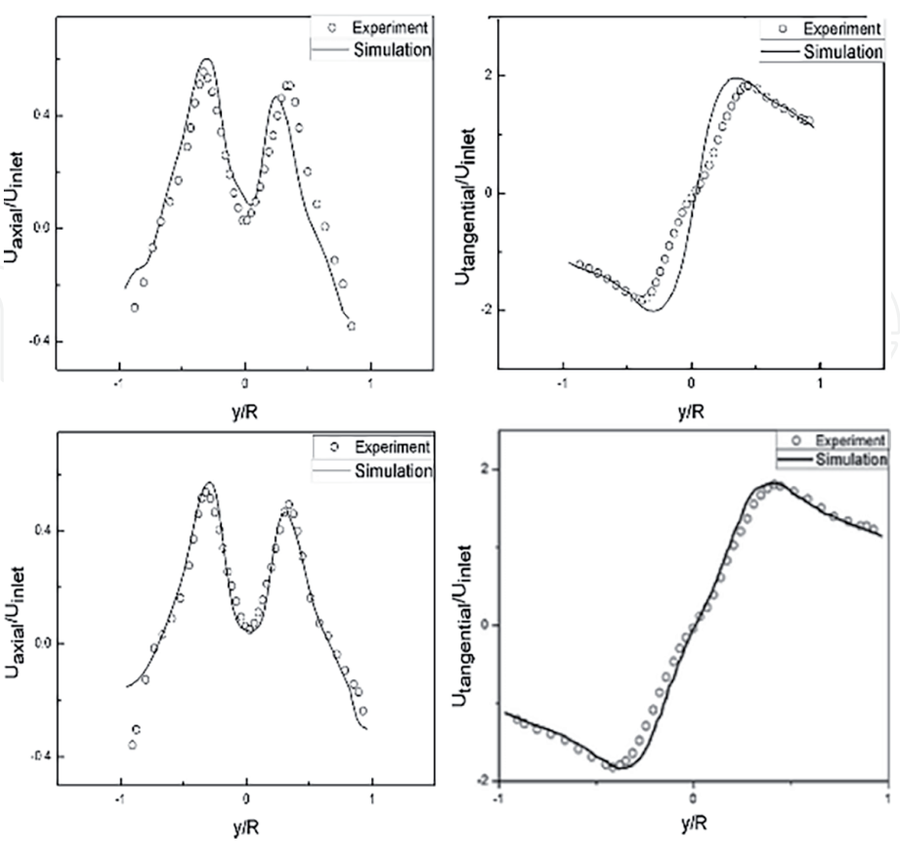

Figure 2.
Comparison of numerically simulated velocity profiles with LDA measurements of Hoekstra [8].

term in the momentum equation is discretized using PRESTO and the momentum terms using QUICK. The turbulent kinetic energy and turbulent dissipation terms are discretized using the first-order upwind scheme.

2.6 Validation

The simulation methodology used in the present study has been validated using the experimental results of Hoekstra [8]. **Figure 2** shows a comparison of the velocity profiles at two axial locations, 0.75D and 2D, generated numerically and through LDA measurements. Good agreement between the velocity profiles is seen and it can be said that the simulations are able to approximate the physical phenomenon with reasonable accuracy.

3. Results and discussion

The results of the two simulation approaches at the four solid concentrations have been analyzed in this section. The mean axial and tangential velocity, profiles at two axial locations (0.75D and 2D from the roof of the cyclone) have already been presented and validated in Section 2.3, and the same flow pattern has been used for injection of particles with different mass loadings.

3.1 Pressure drop

The pressure drop for the clean gas simulation that was run before injecting the particles amounted to 1398.01 Pa but this value increased on injection of particles. Whereas, Fassani and Goldstein [3] and Hoffmann et al. [6] reported the pressure drop to decrease on the introduction of dust particles. Moreover, this reduction was more pronounced at higher inlet velocities. The increase in pressure drop can be attributed to an increase in surface roughness of the cyclone separator walls as particles tend to accumulate towards the walls. **Table 1** shows that the increase in pressure drop for one way coupled simulations is almost same for all the mass loadings with only slight deviations. Whereas for two-way coupling, the pressure drop values are seen to rise marginally with mass loadings. This suggests that due to the increase in mass loadings, the force imparted on the fluid by the particles has a considerable effect on the pressure field inside the cyclone separator. Similar observations were made by Huang et al. [5] and the increased pressure drop was attributed to decrease in gas pressure due to increased wall friction. However, contradictory findings with respect to pressure drop have been reported in the literature [1, 3, 6], which is consistent with the present work for mass loading up to 0.1 kg/kg of gas in

Solids concentration	One-way coupling		Two-way coupling	
	Pressure drop (Pa)	Efficiency (%)	Pressure drop (Pa)	Efficiency (%)
0.05	1492.30	61.88	1486.76	62.50
0.1	1487.20	61.76	1489.24	61.86
0.2	1495.81	61.72	1514.60	66.57
0.3	1503.96	61.63	1558.33	70.31

Table 1.
Pressure drop and separation efficiency values at t = 7.45 s.

one-way coupled simulation. Particle-particle interaction may be the prime reason for reduction in pressure drop for the higher mass loading. In the proposed work mass loading is limited to 0.3 kg/kg of gas for which particle-particle interactions have not been considered. The pressure drop obtained in the proposed work for the considered mass loading ranges matches with Baskakov's model [23].

3.2 Particle motion

Four mass loadings were simulated for the SHEC, The particles were injected into the cyclone after 2.87 s of the start of the fluid flow as it is quite enough for the flow to become steady. Nine particle sizes (8.05×10^{-7}, 1.04×10^{-6}, 1.34×10^{-6}, 1.74×10^{-6}, 2.23×10^{-6}, 2.9×10^{-6}, 3.75×10^{-6}, 4.88×10^{-6}, 6.24×10^{-6} m) were injected into the cyclone and the simulations were run till t = 6.95 s. After which particles still remained in the separation space of the cyclone separator, but were few in number and mainly smaller in diameter. **Figure 3** shows the radial profiles of tangential velocity at three axial locations for mass loadings 0.1 and 0.3. The figure shows that for the mass loadings of 0.1, the tangential velocity distribution for one way and two-way coupled simulations is somewhat similar. This signifies that for such low mass loadings there is hardly any difference between the two simulation strategies thereby confirming the similar pressure drop and collection efficiency values obtained from the two simulation methodologies. But for mass loading of 0.3, the peak tangential velocities for the two-way coupled simulation is seen to decrease this decrease in tangential velocity indicates a change in the flow field and also a decrease in the swirl. It is also observed that this decrease in tangential velocity is more prominent in the free vortex

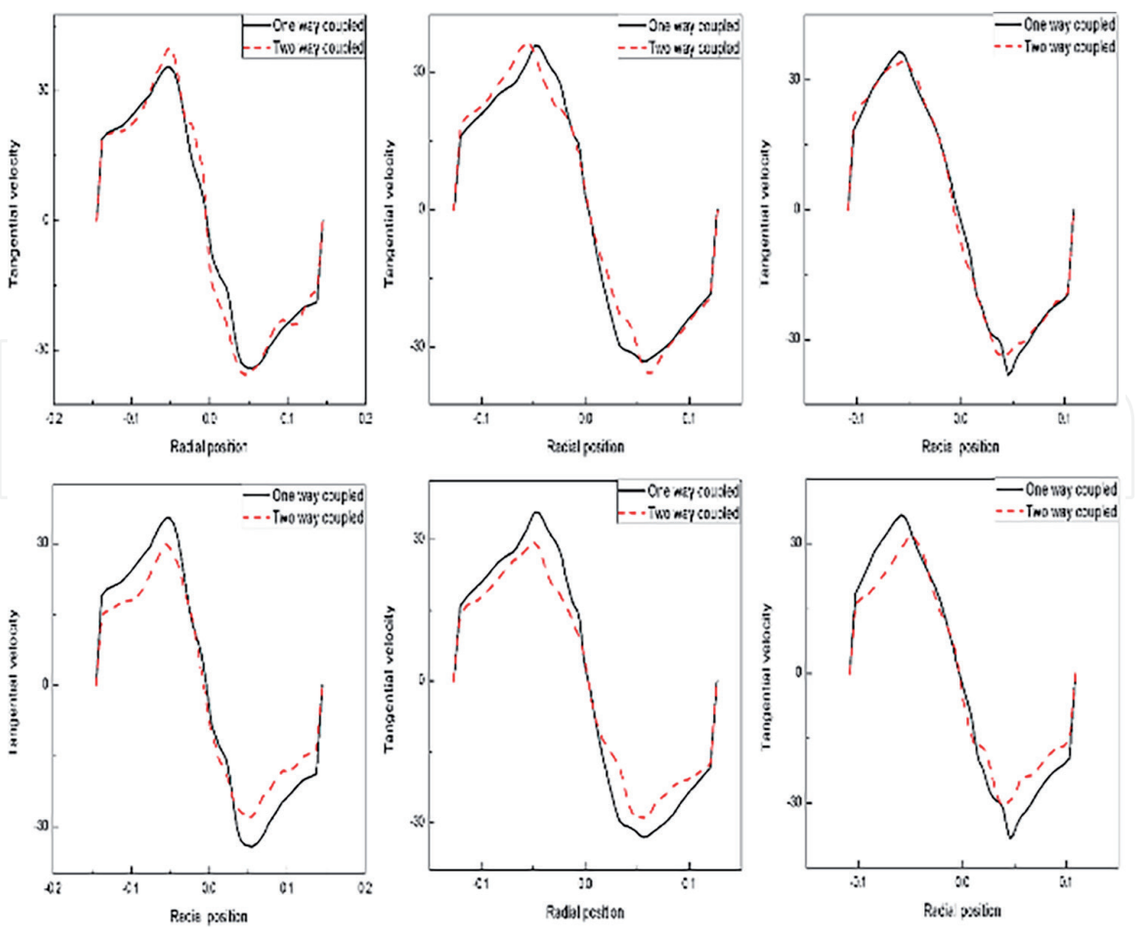

Figure 3.
Radial profiles of tangential velocity top row: mass loading 0.1, bottom row: mass loading 0.3; from left to right: axial location 0.75D, 2D, 2.5D from the cyclone roof.

region where the particles tend to accumulate. Such a behavior has also been observed by Fassani and Goldstein [3]. An interesting observation is that although the swirl reduces, the pressure drop increases though slightly for two-way coupling. This increase in pressure drop can be explained as a result of dominance of increase in wall friction due to presence of a high concentration of particles near the wall as compared to reduction in pressure drop which occurs due to reduction in tangential velocity.

The particles inside the cyclone separator for one way coupling at five instances of time for mass loadings 0.1, and 0.3 are shown in **Figures 4** and **5**. It can be clearly seen that at a later stage in the separation process, only smaller diameter particles are left out in the cyclone and the number of particles left in the cyclone after this time decreases on increasing the mass loadings. Three particle diameters at t = 4.5 s for all the mass loadings are shown in **Figures 6** and 7. The figures confirm that the fate of larger particles is decided very early in the separation process and also that increasing the mass loadings decrease the number of smaller particles left out in the cyclone separator at a later stage. An interesting point seen in **Figures 6** and 7 is that some larger diameter particles are also found stuck in recirculation zones along the annular part of the roof of the cyclone. This gives an idea of the strength of the recirculation zones operating inside the cyclone separator. Comparison of **Figures 6** and 7 shows that at the same time, the number of particles left in the cyclone separator is less for two-way coupled simulations this suggests that the change in flow field brought about by the two-way coupled simulations not only increases the collection efficiency but also decides the fate of particles sooner than that of one way coupling. This was not observed at lower mass loadings than 0.1 but is significantly observed at only mass loadings of 0.3. Two way coupled simulations [5] also showed that the influence of particles on the gas flow field was relatively small at lower mass loadings. This gives an idea of how closely two-way coupling can approximate the real phenomena occurring inside the cyclone separator as compared to one way coupling.

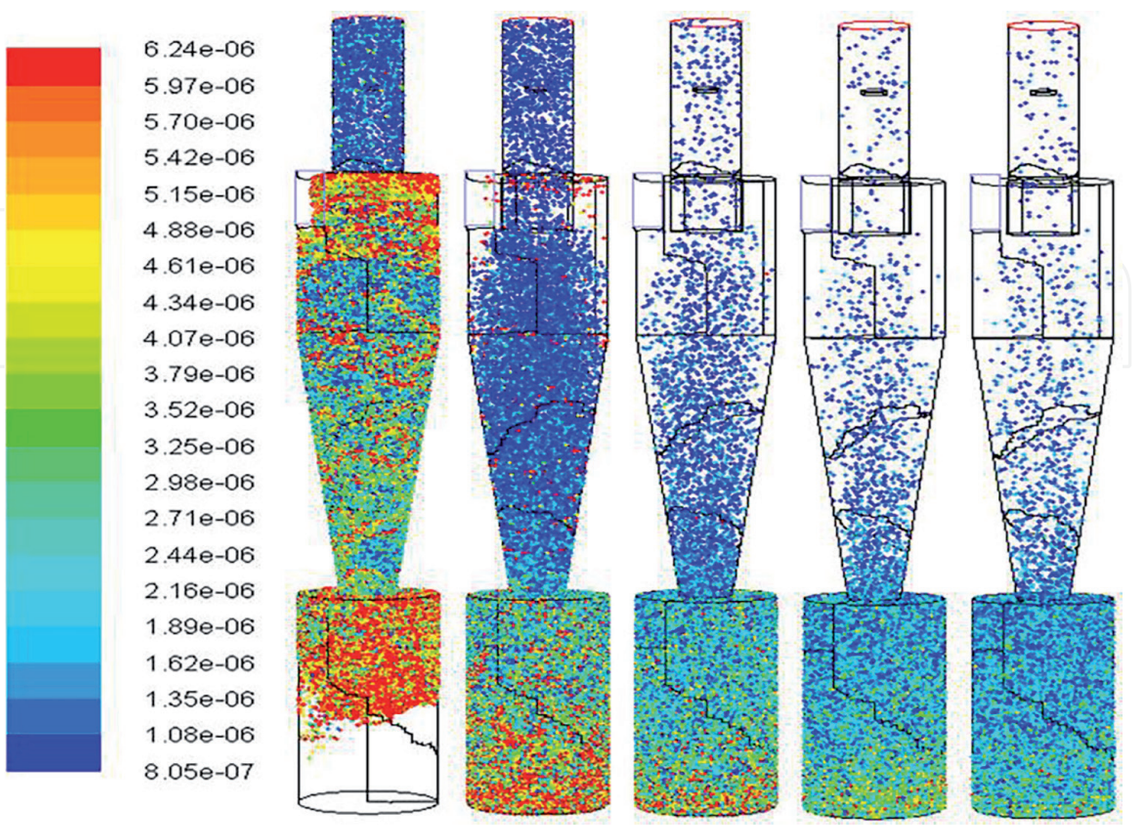

Figure 4.
Particles inside the cyclone from left to right at t = 3.2 s, 3.8 s, 4.5 s, 5.6 s, 6.9 s at mass loadings 0.1.

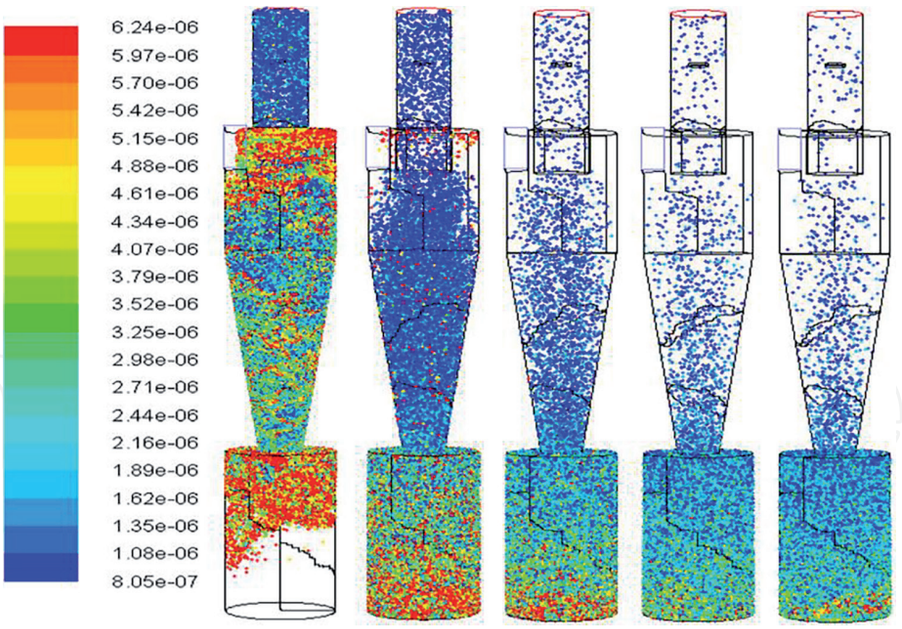

Figure 5.
Particles inside the cyclone from left to right at t = 3.2 s, 3.8 s, 4.5 s, 5.6 s, 6.9 s at mass loadings 0.3.

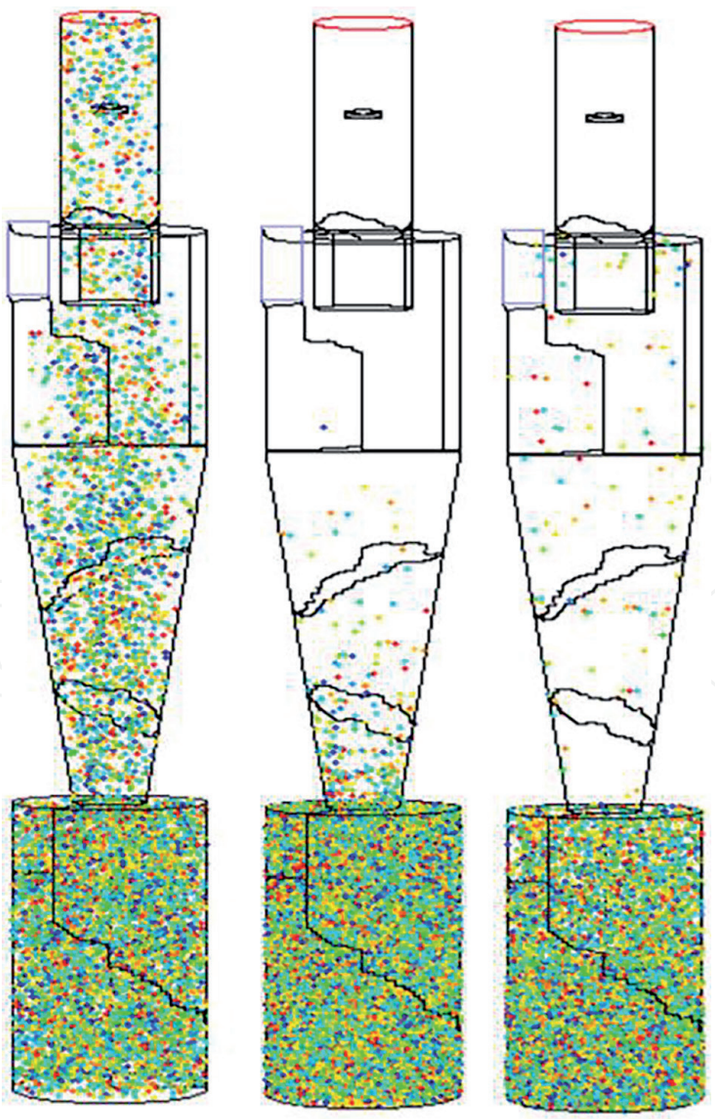

Figure 6.
Single realization of particle sizes 8.05 × 10^{-7}, 2.23 × 10^{-6}, 6.24 × 10^{-6} at t = 4.5 s, for one way coupling at mass loadings 0.3.

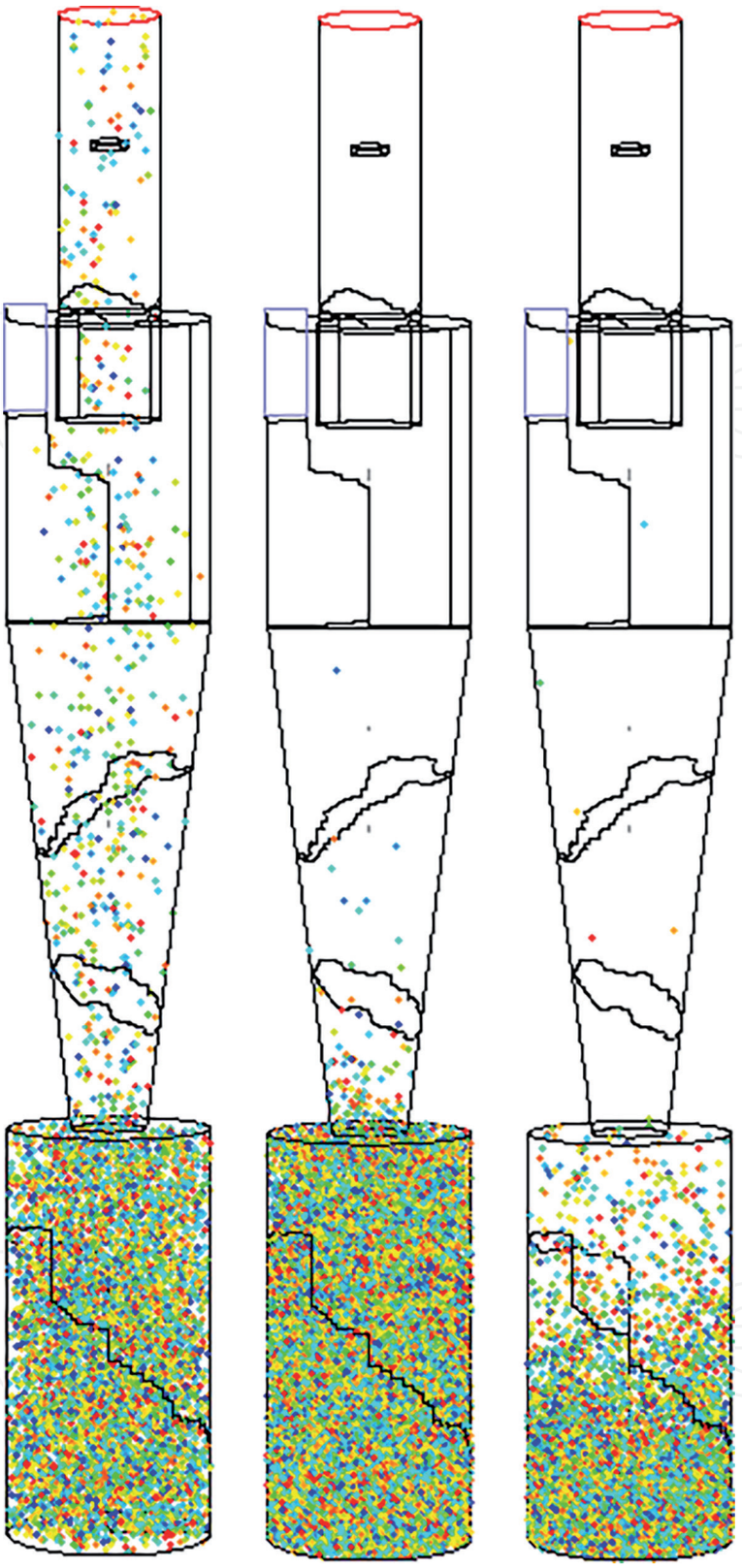

Figure 7.
Single realization of particle sizes 8.05×10^{-7}, 2.23×10^{-6}, 6.24×10^{-6} at t = 4.5 s, for two-way coupling at mass loadings 0.3.

3.3 Collection efficiency

The collection efficiency with respect to mass loadings and the simulation methodology applied at the four mass loadings are given in **Table 1**. **Figure 8** presents both the pressure drop and collection efficiency of the cyclone model at

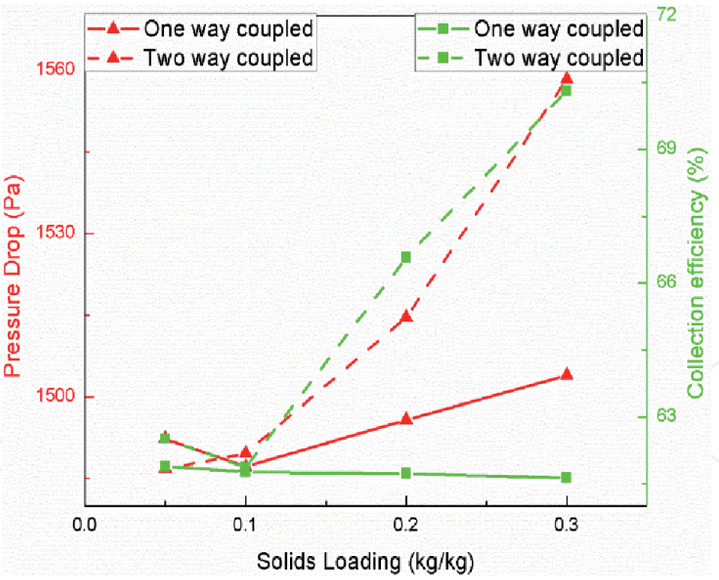

Figure 8.
Pressure drop and collection efficiency obtained at the four solid loadings.

the four solid loadings tested, it is seen that for one way coupled simulations, the pressure drop increases slightly whereas the collection efficiency is seen to decrease marginally. On the other hand, the two way coupled simulations show a marginal increase in the pressure drop and a considerable increase in collection efficiency after the solid loadings increases beyond 0.1. It is observed that one way coupled simulations predicts similar separation capability of cyclone separators at different mass loadings. A similar collection efficiency of the three cases explains the incapability of one way coupled simulations to predict the improvements pointed out by [1]. Therefore the efficiency obtained on considering one way coupled simulations can lead to incorrect estimation of the separation capability at higher mass loadings. Whereas the separation efficiency for two-way coupling can be seen to rise with mass loadings suggesting that the simulation strategy is able to account for the sweeping effect caused by larger particles. Moreover, it is observed that the two strategies of simulation provides similar results till mass loadings of 0.1 but beyond this point, differences in the pressure drop and separation efficiency for both the simulation strategies can be observed. The efficiency obtained by conducting two-way coupled simulations at higher mass loadings is more reliable than one way coupled as the latter does not account for the forces imparted on the continuous phase by the dispersed phase. The fact that any increase in mass of the particles does not have an effect back on the flow and therefore is unable to reduce the swirl.

4. Conclusions

One way and two-way coupled simulations of Stairmand High Efficiency Cyclone at four mass loadings have been performed and the results presented. It can be concluded that

- The two-way coupled simulations are seen to predict the physical phenomena better than the one-way coupled simulations after a solid loading of 0.1.

- At all the solids loadings, a similar separation capability is observed for one way coupling, but for two-way coupling, the separation efficiency and pressure drop are seen to increase with mass loadings. This fact signifies that after a

certain loading condition, one way coupling is not able to correctly capture the effects of the forces that are acting on the continuous phase.

- The collection efficiency of the cyclone model is seen to increase from 62% to 70% on increasing the mass loadings from 0.05 to 0.3 with a marginal increase in pressure drop of only 4.8%.

Acknowledgements

The author would like to thank Dr. Lakhbir Singh Brar, Assistant Professor, B.I.T. Mesra, for his valuable time and help he put in this study.

Conflict of interest

The authors declare no conflict of interest.

Author details

Vikash Kumar* and Kailash Jha
Department of Mechanical Engineering, Indian Institute of Technology (ISM) Dhanbad, Dhanbad, India

*Address all correspondence to: harshvikash@gmail.com

IntechOpen

© 2022 The Author(s). Licensee IntechOpen. This chapter is distributed under the terms of the Creative Commons Attribution License (http://creativecommons.org/licenses/by/3.0), which permits unrestricted use, distribution, and reproduction in any medium, provided the original work is properly cited. CC BY

References

[1] Hoffmann AC, Arends H, Sie H. An experimental investigation elucidating the nature of the effect of solids loading on cyclone performance. Filtration & separation. 1991;**28**(3):188-193

[2] Brar LS, Sharma RP, Dwivedi R. Effect of vortex finder diameter on flow field and collection efficiency of cyclone separators. Particulate Science and Technology. 2015;**33**(1):34-40

[3] Fassani FL, Goldstein L Jr. A study of the effect of high inlet solids loading on a cyclone separator pressure drop and collection efficiency. Powder Technology. 2000;**107**(1-2):60-65

[4] Derksen JJ, Sundaresan S, Van Den Akker HEA. Simulation of mass-loading effects in gas–solid cyclone separators. Powder technology. 2006;**163**(1-2):59-68

[5] Huang AN, Ito K, Fukasawa T, Fukui K, Kuo HP. Effects of particle mass loading on the hydrodynamics and separation efficiency of a cyclone separator. Journal of the Taiwan Institute of Chemical Engineers. 2018;**90**:61-67

[6] Hoffmann AC, Van Santen A, Allen RWK, Clift R. Effects of geometry and solid loading on the performance of gas cyclones. Powder Technology. 1992;**70**(1):83-91

[7] Derksen JJ, Van den Akker HEA, Sundaresan S. Two-way coupled large-eddy simulations of the gas-solid flow in cyclone separators. AIChE Journal. 2008;**54**(4):872-885

[8] Hoekstra AJ. Gas flow field and collection efficiency of cyclone separators. TU Delft. Ph. D. Thesis, Delft University of Technology. 2000

[9] de Souza FJ, de Vasconcelos Salvo R, de Moro Martins DA. Large Eddy Simulation of the gas–particle flow in cyclone separators. Separation and Purification Technology. 2012;**94**:61-70

[10] de Souza FJ, de Vasconcelos Salvo R, de Moro Martins DA. Simulation of the performance of small cyclone separators through the use of Post Cyclones (PoC) and annular overflow ducts. Separation and Purification Technology. 2015;**142**:71-82

[11] Derksen JJ. Separation performance predictions of a Stairmand high-efficiency cyclone. AIChE Journal. 2003;**49**(6):1359-1371

[12] Elsayed K, Lacor C. The effect of cyclone vortex finder dimensions on the flow pattern and performance using LES. Computers & Fluids. 2013;**71**:224-239

[13] Shukla SK, Shukla P, Ghosh P. The effect of modeling of velocity fluctuations on prediction of collection efficiency of cyclone separators. Applied Mathematical Modelling. 2013;**37**(8):5774-5789

[14] Bogodage SG, Leung AY. CFD simulation of cyclone separators to reduce air pollution. Powder Technology. 2015;**286**:488-506

[15] Brar LS, Elsayed K. Analysis and optimization of multi-inlet gas cyclones using large eddy simulation and artificial neural network. Powder Technology. 2017;**311**:465-483

[16] Smagorinsky J. General circulation experiments with the primitive equations: I. The basic experiment. Monthly Weather Review. 1963;**91**(3):99-164

[17] Hinze JO. Turbulence. New York: McGraw-Hill Publishing Co.; 1975

[18] Clift R, Grace JR, Weber ME. Bubbles, Drops, and Particles. New York: Academic Press; 1978

[19] Hoffmann AC, Stein LE, Hoffmann AC, Stein LE. Gas Cyclones and Swirl Tubes. Vol. 56. Berlin Heidelberg New York: Springer-Verlag; 2002

[20] FLUENT, 15.0 User Guide. Fluent Inc. 2015

[21] Stairmand CJ. The design and performance of cyclone separators. Transactions of the Institution of Chemical Engineers. 1951;**29**:356-383

[22] Launder BE, Spalding DB. The numerical computation of turbulent flows. Computer Methods in Applied Mechanics and Engineering. 1974;**3**(2): 269-289

[23] Baskakov AP, Dolgov VN, Goldobin YM. Aerodynamics and heat transfer in cyclones with particle-laden gas flow. Experimental Thermal and Fluid Science. 1 Nov 1990;**3**(6):597-602

IntechOpen